行政院國家科學委員會專題研究計畫　期中進度報告

奈米光電材料與光子晶體基礎研究(2/3)

計畫類別：個別型計畫
計畫編號：NSC94-2112-M-009-015-
執行期間：94 年 08 月 01 日至 95 年 07 月 31 日
執行單位：國立交通大學光電工程學系(所)

計畫主持人：謝文峰

報告類型：精簡報告
報告附件：出席國際會議研究心得報告及發表論文
處理方式：本計畫可公開查詢

中　華　民　國 95 年 5 月 29 日

行政院國家科學委員會補助專題研究計畫□ 成 果 報 告
□x 期中進度報告

奈米光電材料與光子晶體基礎研究(2/3)

計畫類別：□x 個別型計畫　　□ 整合型計畫
計畫編號：NSC93-2112-M-009-035
執行期間： 94 年 08 月 01 日至 95 年 07 月 31 日

計畫主持人：謝文峰
共同主持人：程思誠
計畫參與人員：徐旭政、潘晴如、鄭信民、黃同慶、楊松、吳俊毅、林國峰。
成果報告類型(依經費核定清單規定繳交)：□x精簡報告　□完整報告

本成果報告包括以下應繳交之附件：
□赴國外出差或研習心得報告一份
□赴大陸地區出差或研習心得報告一份
□出席新加坡與日本國際學術會議心得報告及發表之論文各一份
□國際合作研究計畫國外研究報告書一份

處理方式：除產學合作研究計畫、提升產業技術及人才培育研究計畫、列管計畫及下列情形者外，得立即公開查詢
□涉及專利或其他智慧財產權，□一年□二年後可公開查詢

執行單位：國立交通大學光電工程研究所
中　華　民　國 95 年 5 月 20 日

行政院國家科學委員會專題研究計畫成果報告

奈米光電材料與光子晶體基礎研究(2/3)

Fundamental studies on nanophotonic materials and photonic crystals (2/3)

計畫編號：NSC 94-2112-M-009 -015
執行期限：94 年 8 月 1 日至 95 年 7 月 31 日

主持人：謝文峰教授　　國立交通大學光電工程研究所

一、中文摘要

室溫下我們觀察了氧化鋅量子點的能帶工程和聲子空間拘陷現象將會隨量子點之尺寸變化。尺寸縮小造成螢光和吸收光譜藍移顯示量子拘限效應。而由E2聲子被拘限造成的拉曼光譜偏移與不對稱性與由改良空間相關模型之計算結果擬合相當好。

關鍵詞：氧化鋅量子點、寬能隙半導體、能帶工程、量子拘限、聲子空間拘陷、螢光、拉曼散射。

Abstract

Both bandgap engineering and spatial confinement of optical phonon were observed depending upon size of ZnO quantum dots at room temperature. Size-dependent blue shifts of photoluminescence and absorption spectra reveal the quantum confinement effect. The measured Raman spectral shift and asymmetry for the *E*2(high) mode caused by localization of optical phonon agree well with that calculated by using the modified spatial correlation model.

Keywords: ZnO quantum dots, wide-gap semiconductor, band gap engineering, quantum confinement, phonon localization, photoluminescence, Raman scattering.

二、緣由與目的

Recent remarkable crystal growth techniques of nanostructured optical devices operated in the ultraviolet (UV) using zinc oxide (ZnO) as the constituent material[1-4] have prompted studies into the properties of this promising material in its powder and nanocrystilline forms. In nanocrystals, the quantum confinement effect becomes predominant investigation field and gives rise to many interesting electronic and optical properties.[5-11] The phenomena concerning quantum confinement effect in ZnO nanocrystals were rarely studied due to the relatively large electron effective mass caused by the large band gap (3.37eV) of this material. Additionally, the Coulomb interaction of electron and hole has reduced the exciton confinement energy partly due to the small dielectric constant $\varepsilon_{\infty}^{bulk}$ in this system, which is also related to large band gap. Thus, the ZnO binary semiconductor material will have small quantum confinement effect in quantum dot (QD) and quantum well (QW) structures.

ZnO has wurtzite crystal structure which belongs to the space group C_{6v}^{4} and group theory predicts zone-center optical phonon modes are A_1, $2B_1$, E_1 and $2E_2$. The A_1 and E_1 modes and the two *E2* modes are Raman active while the *B* modes are silent. The nonpolar *E*2 phonon modes have two frequencies: *E*2(high) is associated with vibration of oxygen atoms and *E*2(low) is associated with the Zn sublattice. All described phonon modes have been reported in the Raman spectra[12,13] of bulk ZnO. Recently, the Raman spectra always show shift of phonon frequencies in ZnO nanostructures.[14-17] Whether the origin of this shift is due to strain,

intrinsic defects or the size of QDs is still the subject of debates. Nevertheless, by examining ZnO nanocrystals with average sizes of 8.5 and 4.0 nm, Rajalakshmi et al.[17] explained the shift of phonon frequency due to optical phonon confinement in ZnO nanostructures without considering effects of crystallite size distribution (CSD) on the Raman spectra in ZnO nanostructures.

In this report, we present quantum confinement effect revealing blue-shift of absorption and PL spectra with small defect emission for ZnO QDs having the average size varying from 12 to 3.5 nm in diameter. Furthermore, we observed spatial confinement of the optical phonon induces spectral shift, broadening and asymmetry of the *E2*(high) phonon mode by using typical Raman spectroscopy. We also used the modified spatial correlation (SC) model, which takes the CSD into consideration that well fit to the measured Raman spectra.

三、研究方法與步驟

The synthesis of ZnO QDs was carried out using the sol-gel method which is similar to those published elsewhere[18,19]. Stoichiometric zinc acetate dihydrate (99.5% $Zn(OAc)_2$, Riedel-deHaen) was first dissolved into diethylene glycol (99.5% DEG, EDTA). The resultant solution was put in a centrifuge operating 3000 rpm for 30 mins, a transparent solution was then obtained containing dispersive single crystalline ZnO QDs. Finally, the supernatant was dropped on a Si(001) substrate with native oxide and dried at 150℃. The average size of ZnO QDs ranging from 3.5 to 12 nm can be tailored under well-controlled concentration (0.04M-0.32M) of the precursor. The average crystallite size was determined as the previous report[18] using Bede D1 X-ray diffractometer with grazing incidence and JEOL JEM-2100F field emission transmission electron microscope (FETEM) operated at 200 KeV. Micro-Raman spectroscopy was carried out by a frequency-doubled Yb:YAG laser (λ = 515 nm) as a pump source, and detected by a Jobin-Yvon T64000 micro spectrometer with a 1800 grooves/mm grating in the backscattering configuration.

四、結果與討論

Figure 1 shows typical PL and absorption spectra of the samples with different average QD sizes at room temperature. The UV emission represents a relaxed state of exciton near the band edge in the ZnO QDs. The nature of the UV-PL from ZnO QDs itself is still a matter of controversy. Some authors attributed the UV-PL to the recombination of confined excitons,[20] while others argued that the emission comes from surface impurities or defects.[21] In our case, high efficient UV emission near band edge is attributed to confined exciton emission, similar to Ref. (20), with high density of states which shifts to the higher energies from 3.30 to 3.43 eV as the size of QDs decreases from 12 to 3.5 nm which are comparable or smaller than the diameter 4.68 nm of exciton (Bohr radius of bulk ZnO is 2.34 nm)[6]. Additionally, slightly widening in full width at half maximum (FWHM) of UV emission as decreasing ZnO QDs may be caused by the recombination of surface-bound acceptor exciton complexes on the lower energy shoulder.[22] In general, quantum confinement will widen the energy bandgap and give rise to a blue shift in the transition energy as the crystal size decreases. Such a phenomenon also reveals in the absorption spectra, although the faint excitonic absorption peaks due to the moderate size distribution of ZnO QDs. From this figure it can clearly be seen that the absorption onset exhibits a progressive blue shift from 3.43 to 3.65 eV as the size of ZnO QD decreases from 12 to 3.5 nm. We calculated the band gaps by using effective-mass model[18] for different sizes of ZnO QDs and showed good agreement with the experimental data.

In order to observe the optical phonon confinement effect, the measured micro-Raman spectra with different sizes of ZnO QDs are shown in Fig. 2 under a fixed excitation laser power

of 3.1 mW. We can see that the Raman peak at 300 cm^{-1} keeps un-shifted in frequency which comes from Si substrate.[23] On the other side, we found the spectral peak of *E2*(high) optical phonon around 435 cm^{-1} shifting to the lower frequency as decreasing the size of ZnO QDs. Compared with that of the ZnO bulk, a red-shift ranging from 0.8 to 4.7 cm^{-1} was obtained as the QD size decreases from 12 to 3.5 nm. Note that Γ_a and Γ_b are the half widths on the low- and high-energy sides of the *E2*(high) mode. Such a pronouncing shift, broadening, and the asymmetry of the *E*2(high) peak could result from three main mechanisms: (1) phonon localization by intrinsic defects; (2) laser heating in nanostructure ensembles; (3) the spatial confinement within the dot boundaries. The frequency shift of phonon resulting from defects should not depend upon the size of quantum dots and as small defect PL-emission in our samples; therefore, we may exclude the defect phonon-localization. Additionally, no shift to the *E2*(high) peak was observed in all ZnO QDs as the laser power has been varied almost an order of magnitude from 1.5 to 12 mW with a fixed laser spot of about 2 μm^2. As a result, the Raman shift is mainly due to the spatial confinement of optical phonon.

The phonon eigenstates are plane waves with infinite correlation lengths in an ideal crystal, therefore, the Raman scattering can only be observed with phonons around the Brillouin zone center (q = 0) due to the momentum conservation law. As the crystallite is reduced to nano-scale, the momentum conservation law associated with the Raman scattering can be relaxed that leads to the spectral shift, broadening, and asymmetry of the Raman modes. The Raman shift and broadening of ZnMnO nanoparticles[24] had been evaluated based on the SC model[25]. Because the phonon wave function is partially confined to the volume of the crystallite and if the spherical shape of finite size ZnO QDs is assumed, the first-order Raman spectrum $I(\omega)$ can be described by the following equation,[25]

$$I(\omega) \propto \int_0^1 \frac{4\pi q^2 \exp(-q^2 L^2 / 4) dq}{[\omega - \omega(q)]^2 + (\Gamma / 2)^2} \qquad (1)$$

where q is expressed in unit of 2π/a, a is the lattice constant, $\omega(q)$ is the phonon dispersion relation, Γ is the linewidth of *E*2(high) phonon of the ZnO bulk, and L is spatial correlation length corresponding to grain size. Furthermore, Islam et al.[26, 27] reported on the influence of crystallite size distribution (CSD) on the shifts in Raman scattering frequencies and line shapes in silicon nanostructures. They modified the Raman intensity expression, I(ω) of Eq. (1), to I(ω,L_0,σ) by using Guassian CSD of an ensemble of spherical crystallites with mean crystallite size L_0 and standard deviation σ. After integrating the results over the crystallite sizes L under $L_0 > 3\sigma$, the total Raman intensity expression for the whole ensemble of nanocrystallites becomes

$$I(\omega) \propto \int_0^1 \frac{f(q) q^2 \exp(-q^2 L_0^2 / 4) dq}{[\omega - \omega(q)]^2 + (\Gamma / 2)^2}, \qquad (2)$$

where $f(q) = 1/\sqrt{1 + q^2\sigma^2 / 2}$ is the characteristics of the CSD. The calculated normalization Raman profiles from an ensemble of ZnO QDs having a mean crystallite size L_0=6.5 nm with varying σ to illustrate the effect of σ on the Raman line shape are plotted in Fig. 3. It is clear that a single-crystalline component with σ=0.27 describes the Raman spectra of 6.5 nm ZnO QDs quite well. Additionally, the CSD of all samples were about 27%, which agrees with the TEM result,[18] e.g., the obtained crystal size 4.3 nm ± 1.1 nm. The frequency shift $\Delta\omega$ and the asymmetry, Γ_a/Γ_b, of *E*2(high) mode from the ZnO bulk (439cm^{-1}) as a function of diameter or correlation length with σ = 0.27 were plotted in Fig. 4, in which the solid curves the calculated results of the modified SC model and hollow circles for the experimentals. We found the measured frequency shift and asymmetry agrees very well with the calculated ones by the modified SC model and the mean values of crystallite sizes obtained from our fitting are also in

good agreement with the XRD results.

五、結論

In summary, size-dependence of efficient UV photoluminescence and absorption spectra of various ZnO QD sizes give evidence for the quantum confinement effect. We have observed the spectral shift, broadening, and asymmetry of the optical phonons for different sizes of ZnO QDs and clarified the origin of these effects is spatial confinement of phonon in ZnO QDs. Using the modified spatial correlation model to analyze the broadening and asymmetry of the first-order *E*2(high) phonon mode, we further confirmed the phonon confinement based on the finite correlation length of a propagating phonon.

六、自我評估

本年度計畫中我們進行兩部分光電物理之研究，分別為氧化鋅奈米線與量子點之成長與光電性質研究等。我們利用氣相傳輸法成功地在各式基板上成長氧化鋅奈米線，並以溶膠—凝膠法成長氧化鋅量子點。成長之樣品我們分別研究，激子—聲子之交互作用、螢光、受激輻射與雷射現象、拉曼散射等等。在光子晶體波導研究方面，我們發現光子晶體波導的偶合與不偶合現象，並將其應用到雙波長之分光多工器上。這一年來共發表 11 篇光電材料與光子晶體相關的 SCI 論文，及雷射動力學相關研究 SCI 論文計 2 篇，成果還算不錯。

七、 參考文獻

1. L. B. Kong, F. Li, L. Y. Zhang, and X. Yao, J. Mater. Sci. Lett. 17, 769 (1998).
2. R. L. Hoffman, B. J. Norris, and J. F. Wager, Appl. Phys. Lett. 82, 733 (2003).
3. R. Könenkamp, R. C. Word, and C. Schlegel, Appl. Phys. Lett. 85, 6004 (2004).
4. J. B. Baxter, and E. S. Aydil, Appl. Phys. Lett. 86, 053114 (2005).
5. T. Kawazoe, K. Kobayashi, and M. Ohtsu, Appl. Phys. Lett. 86, 103102 (2005).
6. R. T. Senger and K. K. Bajaj, Phys. Rev. B. 68, 045313 (2003).
7. T. A. Klar, T. Franzl, A. L. Rogach, and J. Feldmann, Adv. Mater. 17, 769 (2005).
8. Y. Gu, Igor L. Kuskovsky, M. Yin, S. O'Brien, and G. F. Neumark, Appl. Phys. Lett. 85, 3833 (2004).
9. R. P. Wang, G. Xu and P. Jin, Phys. Rev. B. 69, 113303 (2004).
10. V. V. Ursaki, I. M. Tiginyanu, V. V. Zalamai, E. V. Rusu, G. A. Emelchenko, V. M. Masalov, and E. N. Samarov, Phys. Rev. B. 70, 155204-1 (2004).
11. H. M. Cheng, K. F. Lin, H. C. Hsu, C. J. Lin, L. J. Lin, and W. F. Hsieh, J. Phys. Chem. B. 109, 18385 (2005).
12. J. F. Scott, Phys. Rev. B 2, 1209 (1970).
13. N. Ashkenov *et al.*, J. Appl. Phys. 93, 126 (2003).
14. L. Bergman, X. B Chen, J. L. Morrison, and J. Huso, J. Appl. Phys. 96, 675 (2004).
15. K. A. Alim, V. A. Fonoberov, and A. A. Balandin, Appl. Phys. Lett. 86, 053013 (2005).
16. K. A. Alim, V. A. Fonoberov, M. Shamsa, and A. A. Balandin, J. Appl. Phys. 97, 124313 (2005).
17. M. Rajalakshmi, A. K. Arora, B. S. Bendre and S. Mahamuni, J. Appl. Phys. 87, 2445 (2000).
18. K. F. Lin, H. M. Cheng, H. C. Hsu, L. J. Lin, and W. F. Hsieh, Chem. Phys. Lett. 409, 208 (2005).
19. H. M. Cheng, H. C. Hsu, S. L. Chen, W. T. Wu, C. C. Kao, L. J. Lin, and W. F. Hsieh, J. Cryst. Growth. 277 192 (2005).
20. D. W. Bahnemann, C. Kormann, and M. R. Hoffmann, J. Phys. Chem. 91, 3789 (1987).
21. L. Guo, S. Yang, C. Yang, P. Yu, J. Wang, W. Ge, G. K. L. Wong, Appl. Phys. Lett. 76, 2901 (2000).
22. V. A. Fonoberov and A. A. Balandin, Appl. Phys. Lett. 85, 5971 (2004).
23. R. P. Wang, G. W. Zhou, Y. L. Liu, S. H. Pan, H. Z. Zhang, and D. P. Yu, Phys. Rev. B 61, 16 827 (2000).
24. J. B. Wang, H. M. Zhong, Z. F. Li, and Wei Lu, J. Appl. Phys. 97, 086105 (2005).
25. H. Richter, Z. P. Wang, and L. Ley, Solid State Commun. 39, 625 (1981) and I. H. Campbell and P. M. Fauchet, Solid State Commun. 58, 739 (1986).
26. Md. N. Islam and S. Kumar, Appl. Phys. Lett. 78, 715 (2001).
27. Md. N. Islam, A. Pradhan, and S. Kumar, J. Appl. Phys. 98, 024309 (2005).

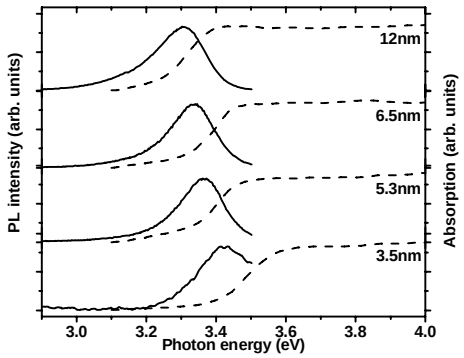

Fig. 1 PL (solid line) and absorption (dashed line) spectra near the band edge of various ZnO QD size.

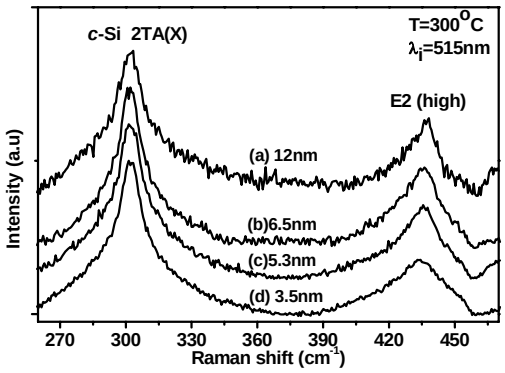

Fig. 2 Typical Raman spectra of different sizes of ZnO QDs: (a) 12nm, (b) 6.5nm, (c) 5.3nm, and (d) 3.5nm.

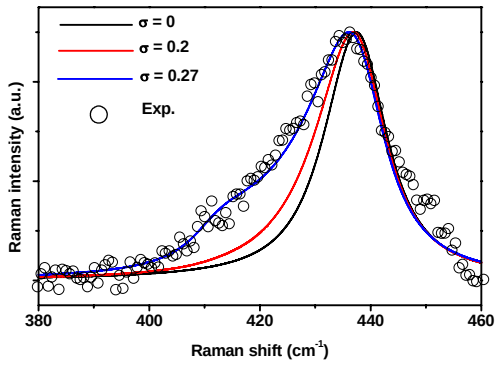

Fig. 3 Fitting of the modified spatial correlation model with σ = 0, 0.2, and 0.27, respectively to the measured result for average size of 6.5 nm ZnO QDs.

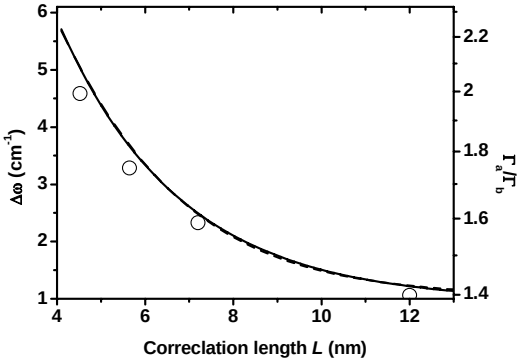

Fig. 4 Raman shift $\Delta\omega$ (solid curve) and asymmetric broadening Γ_a/Γ_b (dashed curve) of *E*2(high) phonon as a function of correlation length L or average size of nanocrystal.